International Journal of Fluid Machinery and Systems
Vol. 4, No. 2, April-June 2011
DOI: 10.5293/IJFMS.2011.4.2.217
ISSN (Online): 1882-9554

Original Paper

The Effect of Casing Geometry on Rotordynamic Fluid Forces on a Closed Type Centrifugal Impeller in Whirling Motion

Julien Richert, Yumeto Nishiyama, Shinichiro Hata, Hironori Horiguchi, and Yoshinobu Tsujimoto

Graduate School of Engineering Science, Osaka University
1-3 Machikaneyama, Toyonaka, Osaka, 560-8531, Japan

Abstract

The rotordynamic fluid forces acting on a closed type impeller in whirling motion were measured and the influence of the clearance geometry on the stability of the impeller was examined. At small positive whirling speed, the rotordynamic forces acted as destabilizing forces for all casings. A small clearance between the shroud of the impeller and the casing caused large fluid force, but did not change the destabilizing region. Radial grooves in the clearance were effective for reducing the fluid forces and destabilizing region due to the reduction of the circumferential velocity without the deterioration of the pump performance. A rotating phenomenon like a rotating stall of the impeller occurred at low flow rate and the resonance between it and the whirling motion led to a sudden increase in force at the whirling speed ratio of 0.7.

Keywords: Pump, Rotordynamic Fluid Force, Whirling Motion, Unsteady Phenomenon

1. Introduction

In high speed turbomachines, the self-excited vibrations of the rotor can be encountered. These vibrations are associated with the rotordynamic fluid forces, induced by the movement of the rotor. Once the overhung rotor exceeds a certain “critical speed”, its movement becomes a combination of whirling and precession motions of increasing amplitude, resulting in flexural stresses and possible contact with the stator. It is therefore common to perform a rotordynamic analysis during the development stage to avoid these problems.

The rotordynamic behavior of closed type impellers has been widely studied in the past. However data on the influence of the clearance between the shroud of the impeller and the casing and especially on the suppressing effect of grooves for whirling motion remain scarce. Thus this study focuses on the measurement of the rotordynamic fluid forces acting on a closed type impeller in whirling motion and the influence of the clearance geometry.

2. Experiment

The experimental facility was already described in previous papers by Yoshida et al. [1] or Suzuki et al. [2] so only a quick overview will be presented here. Figure 1 shows both an overall view of the facility and a detailed view of the mechanism used to impose whirling motion to the shaft. The shaft and impeller are driven by the main motor with a constant rotation speed ω = 41.89 rad/s (400 rpm). The whirling motion Ω is obtained by rotating the sleeve with a servo motor. The sleeve is supported by outer bearings and supports the shaft by inner bearings with an eccentricity of ε. In this study, the value of eccentricity is set constant at ε = 0.6 mm. The whirling speed ratio Ω/ω ranges from -1.2 to 1.2.

The fluid used in this experiment is water at room temperature. From the tank, the water is sucked in the inlet pipe before passing through the impeller, the diffuser and the collector. Two outlet pipes bring back the fluid from the collector to the tank. The flow rate is adjusted by opening or closing symmetrically the two butterfly valves located at the end of the outlet pipes.

Figure 2 displays the schematic of the pump cross-section with the grooved casing with a focus on the front face seal limiting the leakage flow rate in the clearance between the shroud of the impeller and the casing. The gap h in the seal is about 0.4 mm. The shape of the casing is designed so as to keep the clearance C constant. The size of this clearance can be modified by changing the casing. Three casings corresponding to three different clearances were designed and used: C = 5mm (reference), C = 2 mm, C=5 mm with 7 radial grooves. The shape of the grooves can be seen in Figs. 2 and 3. The meridional locations of static and

Received December 10 2010; accepted for publication December 23 2010: Review conducted by Prof. Shuhong Liu. (Paper number O10040C)
Corresponding author: Hironori Horiguchi, Associate Professor, horiguti@me.es.osaka-u.ac.jp

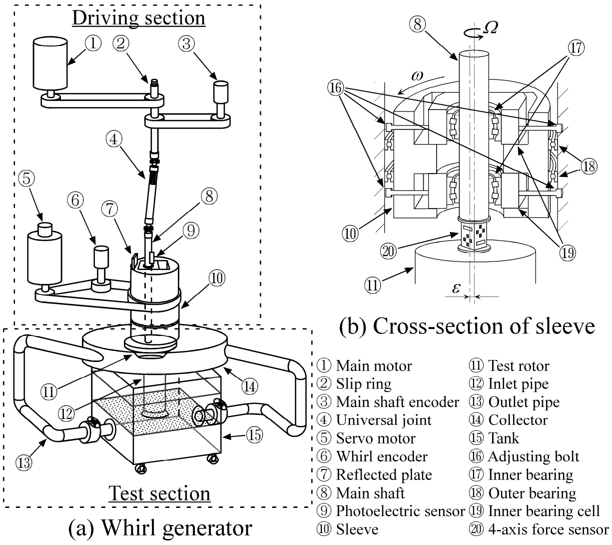

Fig. 1 Experimental facility overview and detail of generator of whirling motion

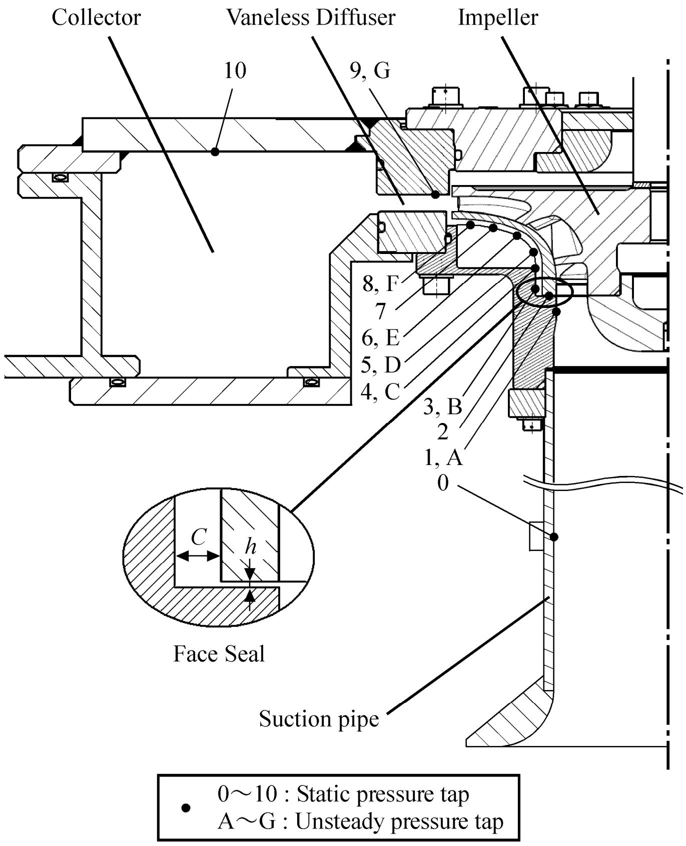

Fig. 2 Schematic of pump cross-section with grooved casing, indicating locations of pressure taps

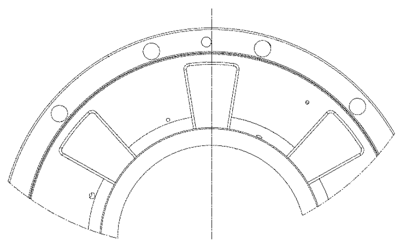

Fig. 3 Upper view of grooved casing

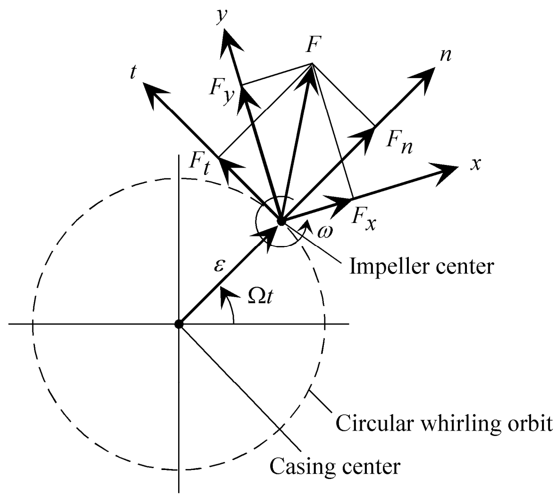

Fig. 4 Coordinate system

Table 1 Specifications of impeller

Outlet radius R_2 [mm]	150
Outlet blade hight b_2 [mm]	10
Outlet blade angle [deg]	80
Blade number (with splitter blades)	18
Face seal clearance h [mm]	0.4

unsteady pressure taps are also shown in Fig.2 by 1-10 and A-G, respectively. The static pressure taps No.0 and 10 are at four different circumferential positions and the pressures at same meridional positions are averaged. Two unsteady pressure taps are set at different circumferential positions in each meridional position to detect the circumferential phase of unsteady phenomena.

The main specifications of the closed type impeller are described in Table1. It can be noted that this impeller is the same model as the open type used by Suzuki et al. [2] with a shroud. The diffuser used here is a vaneless diffuser.

The forces were measured using a 4-axis force sensor mounted directly at the back of the impeller. Figure 4 shows the coordinate system used to define the forces. The coordinates (x,y) is attached to the rotating and whirling impeller. The coordinate (n,t) is attached to the whirling motion. In this representation, it can be noticed that the fluid force tangential to the motion of the impeller F_t is destabilizing if it is in the same direction as the whirling motion, i.e. F_t is destabilizing for $F_t > 0$ for $\Omega/\omega > 0$ or $F_t < 0$ for $\Omega/\omega < 0$. The raw forces measured are the sum of the fluid forces but also the inertia forces of the impeller. To isolate the fluid forces, the inertia forces were measured by running the impeller in the air and then subtracted to the output of the force sensor. Finally, the resulting forces were normalized by the reference force $F_0 = \rho\pi\omega^2 R_2^2 b_2 \varepsilon$.

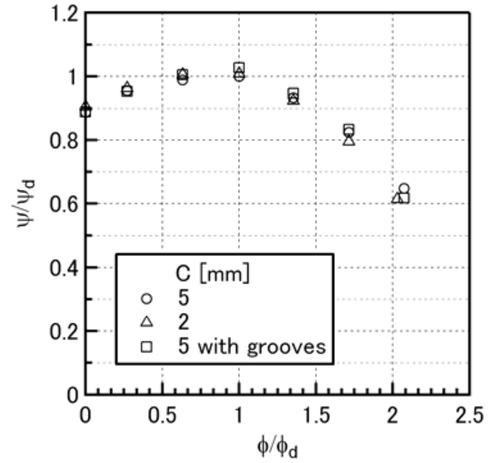

Fig. 5 Performance curve

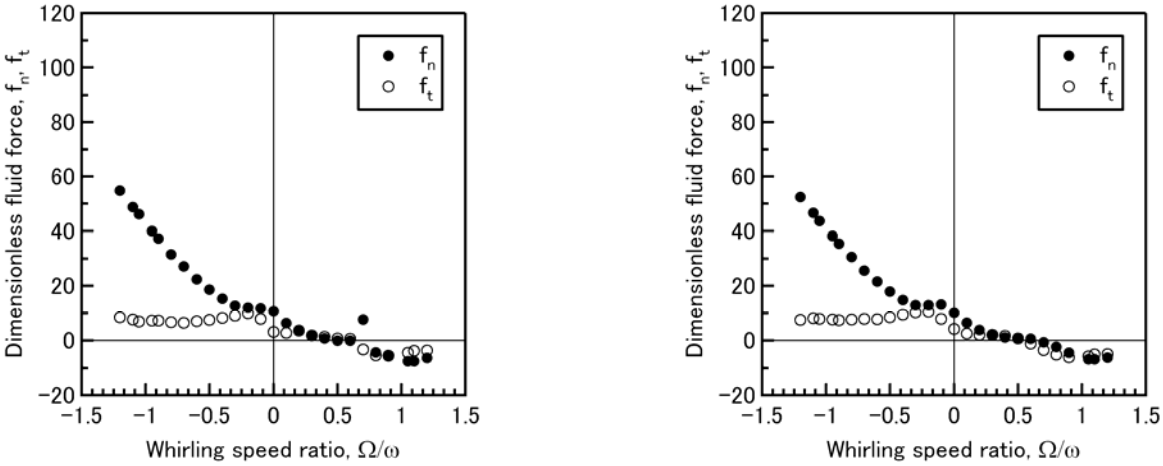

(a) ϕ=0.7ϕ_d

(b) ϕ=ϕ_d

Fig. 6 Normal and tangential fluid forces for *C*=5mm

3. Results and Discussions

3.1 Performance Curve

Static pressure measurements for the performance curve were done with the impeller in eccentric position (ε = 0.6 mm) and with a small whirling speed (Ω/ω = 0.05) in order to reduce the effect of asymmetric positioning of the impeller after averaging the recorded data. The inlet pressure tap is located at the inlet of the suction pipe as shown in Fig.2 (Position 0). The outlet tap is located in the upper wall of the collector (Position 10).

Figure 5 shows the performance curves for each casing. The three curves are very similar indicating that there is little effect of the clearance shape on the pump performance.

3.2 Rotor Dynamic Fluid Forces

This section presents the nondimensional normal and tangential rotordynamic fluid forces f_n and f_t measured with each of the three different casings and for two different flow rates: at low flow rate, ϕ =0.7ϕ_d and at design flow rate, ϕ =ϕ_d. Forces were also recorded for higher flow rates but there is no visible change. Therefore these data are not presented here. The casing with C = 5 mm used as the reference casing has the same features as the grooved casing displayed in Fig.2 except that there are no grooves.

In Figs. 6(a) and (b) are presented the fluid forces for the casing with C = 5 mm at the two flow rates. The general trend observed is a quadratic shape of the normal forces f_n. The tangential forces f_t have a roughly linear behavior. These trends can be found for the cases of shrouded centrifugal impellers [3].

It can be noticed that there is nearly no effect of the flow rate on the forces except for a jump in normal force at Ω/ω = 0.7 at low flow rate. It seems singular but it has a good repeatability and a similar phenomenon has also been reported in the previous study for the open type impeller [2], though it was larger in amplitude and range. This phenomenon can be caused by a resonance of the rotating stall in the impeller with the whirling motion [4]. To confirm its nature, unsteady pressure measurements were done at the inlet and outlet of the impeller as well as in the clearance (Position A to G in Fig.2). The spectrum of pressure fluctuation at

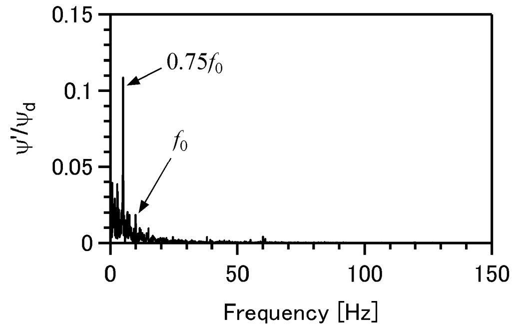

Fig. 7 Spectrum of normalized pressure fluctuation in reference clearance at Position A for ϕ=0.7ϕ_d and Ω/ω=0

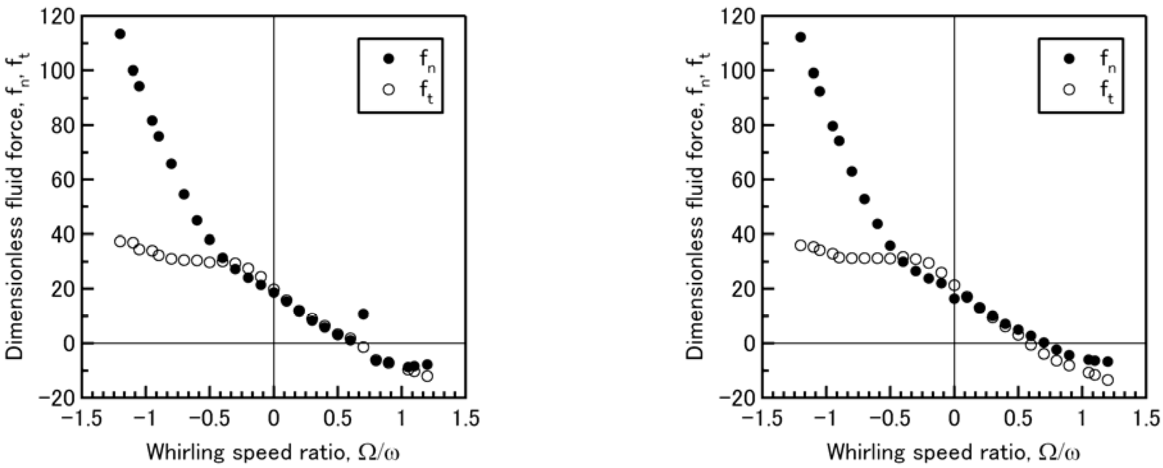

(a) ϕ=0.7ϕ_d (b) ϕ=ϕ_d

Fig. 8 Normal and tangential fluid forces for C=2mm

Position A for ϕ =0.7 ϕ_d is shown in Fig.7. The peak of 5 Hz (≈ 0.75 f_0, f_0=6.67Hz) can be observed. The presence of a second transducer at the same meridional position let us measure the phase. It was the same value as the angle between the two pressure sensors. These observations confirmed the rotating nature of the phenomenon and the possible resonance between it and the whirling motion, leading to a sudden increase in force at Ω/ω = 0.7 for low flow rate. This phenomenon is thought to be a rotating stall in the impeller because the larger pressure fluctuation was observed at the inlet of the impeller and its frequency is in the normal range for rotating stall appearance in impellers. Unsteady computation is being conducted to identify this phenomenon.

The forces for the casing with C = 2 mm at low and design flow rates are displayed on Figs. 8(a) and (b). These figures show the same trend as in the reference case of larger clearance (C = 5 mm). However the level of the forces is more than twice that of the forces in the case of C = 5 mm, especially in Ω/ω < 0.5. Guinzburg et al. [5] pointed out that the magnitude of the forces is roughly inversely proportional to the clearance. This comment is reasonable in our experiment. The destabilizing region of Ω/ω did not change due to the clearance, though the destabilizing region is larger with a smaller clearance in the study of Ref. [5]. We can notice again the presence of the increase in normal force at Ω/ω = 0.7 for low flow rate.

It is known that radial grooves or ribs located on the casing wall in the clearance between the casing and the shroud of the impeller are effective to reduce the circumferential velocity and the destabilizing region of Ω/ω for whirling motion [6]-[8]. In the present study, the grooved casing shown in Figs. 2 and 3 was tested to reduce the destabilizing region. The casing has seven large grooves and the clearance C is 5 mm.

Figures 9(a) and (b) show the fluid forces for the grooved casing with C = 5 mm at low and design flow rates. The difference in the normal force is remarkable with a large decrease compared to the results of the reference casing. The tangential force also decreased though in a less dramatic way. This change is noticeable at low whirling speed and goes with a slight decrease of the destabilizing region f_t >0 when Ω/ω >0.

Figure 10 shows the pressure coefficient ψ_L/ψ_d at Position 0-10 shown in Fig.2. The values of ψ_L/ψ_d for the grooved casing are larger than those for the casings without grooves. This indicates that the grooves successfully decreased the circumferential velocity.

The previously observed jump in normal force at Ω/ω = 0.7 does not appear this time at low flow rate. However there still seems to be a disturbance around that whirling speed but with a decreasing trend in forces. It may indicate that the grooves have some influence on the rotating phenomenon.

As said before, unsteady pressure measurements were done in the clearance. In addition to the phenomenon of 5 Hz (≈ 0.75 f_0) for low flow rates, a phenomenon of 38 Hz (≈ 5.8 f_0) was present in all cases for all flow rates. The magnitude of its pressure fluctuation was larger in the clearance. Figure 11 shows the spectrum of pressure fluctuations at Position E as shown in Fig.2 for

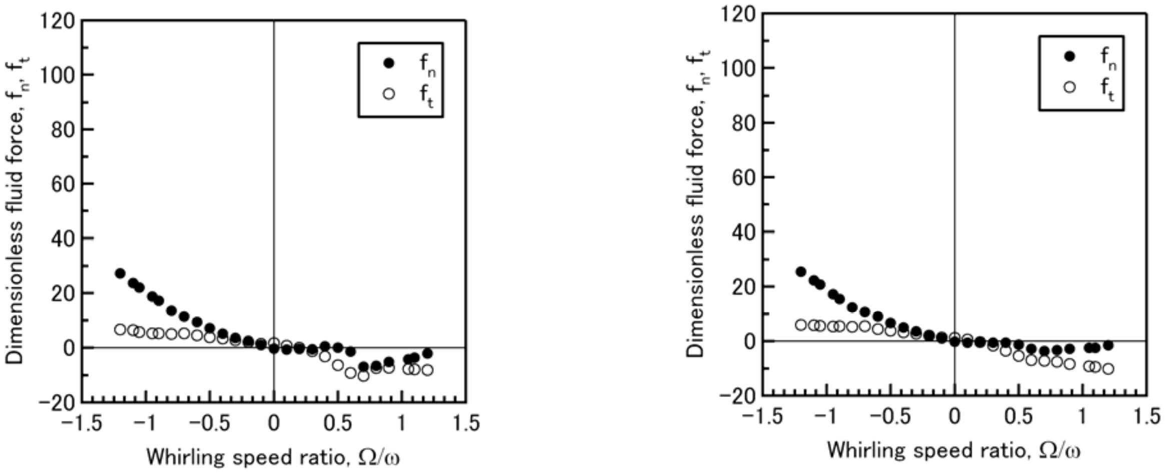

(a) ϕ=0.7ϕ_d (b) ϕ=ϕ_d

Fig. 9 Normal and tangential fluid forces for *C*=5mm with grooved casing

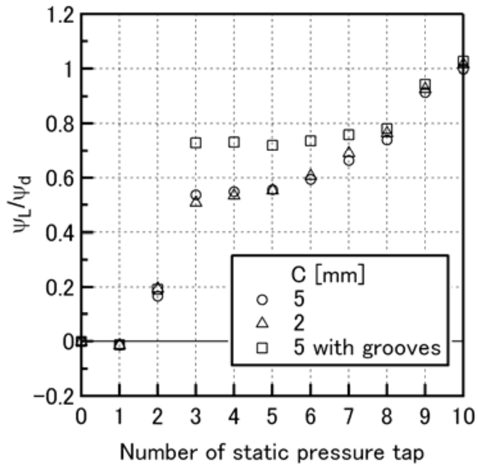

Fig. 10 Comparison of pressure distribution in clearance for ϕ=ϕ_d and Ω/ω=0

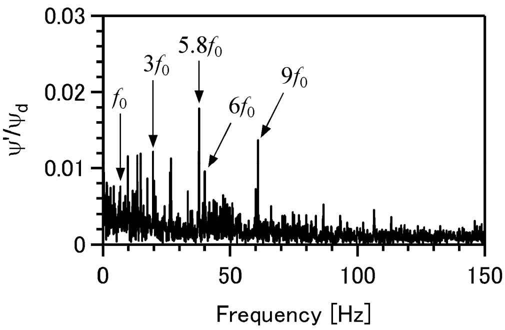

Fig. 11 Spectrum of normalized pressure fluctuation in reference clearance at Position E for ϕ=ϕ_d and Ω/ω=0

the reference casing at $\phi = \phi_d$ and $\Omega/\omega = 0$. The amplitude of 38 Hz (≈ 5.8 f_0) is larger than that of the main blade passing frequency (9 f_0). The phase study showed that the phenomenon is of meridional nature (phase around 0 degrees at $\phi = \phi_d$) but with variations due to the flow rate. First unsteady computations also showed the presence of such a phenomenon leading to the idea this may be some oscillation mode of the flow rate in the clearance. Further research is necessary to clarify the generation mechanism of this phenomenon.

4. Conclusions

In this study, the fluid forces acting on a closed type impeller with various clearance geometries were measured and commented. These results can be summarized as follows:
(1) Rotordynamic forces are destabilizing at small positive whirling speed for all casings.
(2) A decrease of the clearance causes the fluid forces to increase dramatically. The destabilizing region did not change.
(3) Grooves in the clearance are effective for reducing the fluid forces and destabilizing region without decrease of the pump performance.
(4) A rotating phenomenon of 5 Hz (≈ 0.75 f_0) appearing only at low flow rates was identified and is thought to correspond to the rotating stall of the impeller.
(5) A phenomenon of 38 Hz (≈ 5.8 f_0), which seemed to be a flow rate oscillation in the clearance in the meridional direction, was observed both in experiment and in unsteady computations.

Acknowledgement

The authors would like to thank undergraduate student Yutaro Wada for his help during the experiment.

Nomenclature

b_2	Outlet blade height	u_2	Outlet blade tip velocity
C	Front face clearance	ε	Eccentricity of the shaft
f_0	Frequency of shaft rotation, 6.67[Hz] (400[rpm])	ϕ	Flow coefficient, $Q/(2\pi\omega R_2^2 b_2)$
		ϕ_d	Design flow coefficient
f_n	Dimensionless normal fluid force, F_n / F_0	ρ	Water density
f_t	Dimensionless tangential fluid force, F_t/F_0	ω	Angular velocity of the shaft, 41.89[rad/s] (400[rpm])
F_0	Reference force, $\rho\pi\omega^2 R_2^2 b_2 \varepsilon$		
F_n	Normal fluid force	Ω	Angular velocity of the whirling motion
F_t	Tangential fluid force	Ω/ω	Whirling speed ratio
h	Front face seal gap	ψ	Pressure coefficient, $(P_{out}-P_{in})/(\rho u_2^2)$
P	Pressure	ψ_d	Reference pressure coefficient, ψ for the reference casing with C=5mm at the design flow rate
P_{in}	Pressure at Point 0 in Fig.2		
P_{out}	Pressure at Point 10 in Fig.2		
$\lvert \tilde{P} \rvert$	Amplitude of fluctuating pressure	ψ_L	Local pressure coefficient, $(P-P_{in})/(\rho u_2^2)$
Q	Volumetric flow rate	ψ'	Pressure fluctuation coefficient, $\lvert \tilde{P} \rvert/(\rho u_2^2)$
R_2	Outlet radius of the impeller		

References

[1] Yoshida, Y., Tsujimoto, Y., Ishii, N., Ohashi, H. and Kano, F., 1999, “The Rotordynamic Forces on an Open-Type Centrifugal Compressor Impeller in Whirling Motion,” ASME, Journal of Fluids Engineering, Vol. 121, pp. 259-265.

[2] Suzuki T., Prunieres, R., Horiguchi, H. and Tsujimoto, Y., 2008, “Experimental Measurement of Rotordynamic Fluid Forces on an Open-Type Impeller in Whirling Motion,” ISROMAC 12-2008-20131, pp. 1-7.

[3] Jery, B., Brennen, C.E., Caughey, T.K. and Acosta, A., 1985, “Forces on Centrifugal Pump Impellers,” Proceedings of the Second International Pump Symposium, pp. 21-29.

[4] Tsujimoto, Y., Acosta, A.J. and Brennen, C.E., 1986, “A Theoretical Study of Impeller and/or Vaneless Diffuser Attributed Rotating Stalls and Their Effects on the Whirling Instability of a Centrifugal Impeller,” Transactions of the JSME, Series B, Vol. 52, No. 483, pp. 3747-3754, (In Japanese).

[5] Guinzburg, A., Brennen, C.E., Acosta, A.J. and Caughey, T.K., 1994, “Experimental Results for the Rotordynamic Characteristics of Leakage Flows in Centrifugal Pumps,” ASME, Journal of Fluids Engineering, Vol. 116, pp. 110-115.

[6] Ohashi, H., Sakurai, A. and Nishihama, J., 1988, “Influence of Impeller and Diffuser Geometries on the Lateral Fluid Forces of Whirling Centrifugal Impeller,” NASA Conference Paper 3026, pp. 285-306.

[7] Sivo, J.M., Acosta, A.J., Brennen, C.E. and Caughey, T.K., 1995, “The Influence of Swirl Brakes on the Rotordynamic Forces Generated by Discharge-to-Suction Leakage Flows in Centrifugal Pumps,” ASME, Journal of Fluids Engineering, Vol. 117, pp. 104-108.

[8] Hsu, Y. and Brennen, C.E., 2002, “Effect of Swirl on Rotordynamic Forces Caused by Front Shroud Pump Leakage,” ASME, Journal of Fluids Engineering, Vol. 124, pp. 1005-1010.